Asian Journal of Chemistry; Vol. 38, No. 7 (2026), 1759-1767
ASIAN JOURNAL OF CHEMISTRY
https://doi.org/10.14233/ajchem.2026.35891

Seasonal Dynamics of Jarosite-Rich Residue Crystallinity and Its Implications for Heavy Metal Mobility, Bioavailability and Crop Uptake in Semi-Arid Agricultural Soils

VASEEM AKHTAR[1], KIRTI MOHAN SHARMA[1,*] and DINESH KULHARY[2]

[1]Department of Chemistry, Career Point University, Kota-325003, India
[2]Department of Chemistry, Swami Keshvanand Institute of Technology, Management & Gramothan, Jaipur-302017, India

*Corresponding author: E-mail: kirtimohansharma@gmail.com

Received: 7 March 2026 *Accepted*: 23 May 2026 *Published online*: 3 July 2026 AJC-22401

Jarosite residue, a secondary sulphate mineral prevalent in acid mine drainage (AMD) systems and hydrometallurgical zinc-processing wastes, serves as a transient repository for heavy metals such as lead (Pb), arsenic (As), cadmium (Cd) and zinc (Zn). However, its stability is profoundly influenced by the seasonal environmental fluctuations. This study reports the crystal-chemical transformations of jarosite rich industrial waste across wet (monsoon) and dry seasons, elucidating their ramifications for heavy metal mobility, soil contamination, crop bioaccumulation and human health risks. Soil and waste samples were collected from a jarosite residue dump (site A), adjacent agricultural soil (site B) and a reference site (site C) during peak dry (March 2025) and wet (July 2025) seasons. Analyses encompassed physico-chemical properties (pH, EC, organic carbon, CEC), X-ray diffraction for mineralogy, ICP-MS for total and bioavailable metals, BCR sequential extraction for speciation, batch dissolution experiments simulating seasonal conditions, crop metal accumulation in wheat and maize, bioaccessibility assessments and pilot remediation trials using lime, biochar and bentonite. Results revealed heightened jarosite residue dissolution and reduced crystallinity (from 0.87 to 0.80) in the dry season, fostering transformation to goethite and anglesite, with Pb and As shifting from residual (65-75%) to labile fractions (45-55%). Bioavailable Pb and As at site A surged from 5.59 and 2.08 mg/kg (wet) to 19.52 and 7.74 mg/kg (dry), respectively. Batch experiments confirmed amplified metal release (up to 70% Pb, 54% As) at elevated temperatures (45 ºC) and pH 7.5. Crop grains from site B exhibited elevated accumulation (*e.g.* 2.5 mg/kg Pb in wheat), yielding hazard quotients exceeding 1 for children, indicating non-carcinogenic risks. Remediation amendments reduced bioavailable metals by 55-65%, enhancing pH and CEC. These findings underscore the vulnerability of semi-arid mining ecosystems to seasonal dynamics, encouraging tailored waste management and bioremediation strategies to mitigate contamination and foster sustainable agricultural practices in affected regions.

Keywords: Jarosite residue, Heavy metal mobility, Industrial waste, Seasonal dynamics, Rajasthan soils, Acid mine drainage.

INTRODUCTION

Jarosite residue [$KFe_3(SO_4)_2(OH)_6$] is the typical secondary mineral in the acid mine drainage (AMD) systems and industrial wastes generated in the course of hydrometallurgical processing of zinc [1]. Jarosite residue is an acidic sulphate-rich mineral and a major environmental geochemistry player since it has the capacity to sequester heavy metals and metalloids, including lead (Pb), arsenic (As), cadmium (Cd) and zinc (Zn) in its crystal structure by either substitution or adsorption [2]. This entrapment makes jarosite residue a short-term trap of toxic pollutants, which lowers the immediate bioavailability of the pollutants in mining-affected waters. However, the stability of jarosite residue is highly susceptible to the environmental factors like pH, temperature, redox potential and moisture which fluctuate seasonally particularly in semi-arid regions like the Dariba mining district in the state of Rajasthan, India [3]. These changes may cause the dissolution or conversion to other secondary phases [*e.g.* goethite (α-FeO(OH) or anglesite ($PbSO_4$)] that may release sequestered heavy metals to the surrounding soils and water bodies, which has a high environmental and health risk [4,5].

Dariba mining area, one of the largest zinc and lead mining regions of India, has been generating large amounts of jarosite residue-rich wastes as byproducts of hydrometallurgical zinc recovery. This waste is normally buried in landfills or open dumps and is exposed to the soils and hydrological systems of the area, which can cause pollution of the area due to the

movement of the leachate [1,6,7]. The semi-arid climatic conditions of the region, the extreme variations in temperature (10 ºC in winter and 45 ºC in summer) and the concentrated monsoon precipitation (600-800 mm per annum) makes the region an active environment, which influences the crystal-chemical behaviour of jarosite residue. During the dry season, the arid terrain and hot weather may promote dehydration of minerals and lattice dissolution, but in the monsoon seasons, the dissolution or leaching may be promoted, which may affect the mobility of heavy metals [7]. Such seasonal processes are critical to long-term environmental impacts of the jarosite residue in the sense that they will define the equilibrium between metal sequestration and release, which has implications on the soil quality, groundwater safety and ecosystem health.

Jarosite-rich waste has become a major problem in mining areas all over the world and has been found to cause soil and water contamination in places like Spain, Australia and China [8,9]. This is made worse by the fact that the waste dumps in Dariba are near agricultural lands and heavy metals that might be released by jarosite residue concentrated in crops and thus enter the food chain and cause health hazards [6]. As has been previously noted, jarosite residue has been noted to have a dual nature of being a scavenger and a source of heavy metals and its behaviour is dependent upon environmental conditions [10]. Nevertheless, there is a paucity of research examining seasonal changes of the crystal-chemical characteristics of jarosite residue and their individual effects on the mobility of heavy metals in semi-arid mining areas such as Dariba. Such knowledge is essential in the prediction of high-risk phases of contamination and site-specific and locally oriented remediation strategies that are dependent on local climatic conditions. This gap is tried to be filled in the present [5] recorded at the solution surface at exactly 40 sec (R1st) and 8 h (R2nd).

EXPERIMENTAL

Characterisation: Mineralogical analysis was conducted using X-ray diffraction (XRD) on a Bruker D8 Advance diffractometer with Cu*K*α radiation (λ = 1.5406 Å). Prior to analysis, Samples were air-dried at 25 ºC, ground to < 63 μm using an agate mortar. Powdered samples were mounted as randomly oriented specimens and scanned from 5º to 70º 2θ at a step size of 0.02º and a scan speed of 1º/min. Phase identification was performed using the Joint Committee on Powder Diffraction Standards (JCPDS) database. Semi-quantitative phase analysis was performed using Rietveld refinement, in which peak profile functions were iteratively refined for jarosite residue and associated mineral phases [11]. The full width at half maximum (FWHM) and relative peak intensity of the main diffraction peaks were used to assess the crystallinity of jarosite residue of jarosite. Using OriginPro software, the ratio of crystalline peak area to total peak area was used to determine the crystallinity index (CI). Using the Rietveld refinement method and X'Pert HighScore software, peak fitting and refinement were carried out [12]. The ratio of crystalline peak area to total diffraction area was used to determine the crystallinity index (CI) of jarosite residue from XRD patterns:

$$\text{Crystallinity index (CI)} = \frac{A_c}{A_c + A_a}$$

where A_c is the integrated crystalline diffraction peak area and A_a is the amorphous background. Origin2018 implemented baseline subtraction, peak deconvolution and area integration. Gaussian–Lorentzian functions suited jarosite's characteristic diffraction peaks, whereas X'Pert HighScore Plus performed phase identification and Rietveld refining. Under seasonal environmental stress, lower CI values suggest partial amorphisation and structural deterioration, whereas higher values imply structural ordering and mineral durability.

Physico-chemical analysis: Cation exchange capacity (CEC) was measured using the ammonium acetate method (pH 7.0) to assess metal retention capacity of soil [13]. The soil samples (0.5-10 g) were saturated with 25 mL NH_4OAc (1 M, pH-7) solution. After shaking and subsequent centrifugation, the supernatant was collected for analysis of exchangeable cations. The residues were then washed with 30 mL ethanol (97%) and centrifuged and the supernatant was discarded. This was repeated to total three washes. After discarding the last ethanol, the tubes with soil were weighed to calculate entrained ethanol mass in the soil and samples were saturated with 30 mL KCl (1 M). The samples were shaken and subsequently centrifuged. The supernatant was analysed for NH_4-N. The CEC values were calculated from the measured molar concentration of NH_4-N in the supernatant after correction for the volume of entrained ethanol.

Chemical analysis: Total concentrations of Fe, Pb, Zn, As and Cd were determined using inductively coupled plasma mass spectrometry (ICP-MS, Agilent 7900) after aqua regia digestion (ISO 11466) of the samples. In brief, 0.5 g of sample was digested in 12 mL aqua regia (3:1 HCl:HNO_3) at 95 ºC for 2 h, filtered and diluted to 50 mL with deionised water. Calibration was performed using multi-element standards, with detection limits of 0.01 mg/kg for Pb, As and Cd and 8 mg/kg for Zn [1]. Bioavailable fractions were extracted using 0.01 M $CaCl_2$ (1:10 soil: solution ratio, shaken for 2 h at 25 ºC), filtered (0.45 μm) and analysed *via* ICP-MS [14]. The BCR sequential extraction procedure was applied to categorize metals into four fractions: (i) acid-soluble (0.11 M acetic acid), (ii) reducible (0.5 M hydroxylamine hydrochloride), (iii) oxidizable (1 M ammonium acetate after H_2O_2 digestion) and (iv) residual (aqua regia digestion) [14]. Each extraction step was performed in triplicate and recoveries were validated against certified reference materials (CRM BCR-701).

Batch dissolution experiments: Batch dissolution experiments were conducted to simulate seasonal conditions (pH 5.5-7.5, 10-45 ºC) and evaluate jarosite residue stability and metal release. Synthetic K-jarosite residue was prepared following Drouet & Navrotsky [15] by dissolving $Fe_2(SO_4)_3$ and K_2SO_4 in deionised water at 95 ºC and pH 1.5, followed by filtration and drying. Experiments used 1 g of sample (field or synthetic jarosite residue) in 50 mL of deionised water, with pH adjusted using 0.1 M NaOH or HCl. Solutions were agitated at 150 rpm in a temperature-controlled shaker (10 ºC for wet season, 45 ºC for dry season). Aliquots were sampled at 24 and 48 h, filtered (0.45 μm) and analysed for dissolved Pb, Zn, As and Cd *via* ICP-MS.

Crop sampling and metal bioaccumulation analysis: To assess heavy metal accumulation in local crops, samples were collected from agricultural fields adjacent to the jarosite residue-rich waste dump, wheat (*Triticum aestivum*) during the dry (March 2025) and maize (*Zea mays*) (site B) during the wet (July-August 2025) seasons. At each site, five composite samples of mature grains were collected from 1 m^2 area, oven-dried at 60 ºC and ground to < 0.5 mm. Samples (0.5 g) were digested using a 3:1 HNO_3:$HClO_4$ mixture at 120 ºC for 3 h, filtered and analysed for Pb, As, Cd, Cu and Ni *via* ICP-MS [12]. Bioaccessibility of metals, reflecting potential human uptake *via* ingestion, was evaluated using the simple bioaccessibility extraction test (SBET). A 0.4 M glycine solution (pH 1.5) was used to simulate gastric conditions, with 1g of crop sample extracted at 37 ºC for 1 h, followed by filtration and ICP-MS analysis [16]. Human health risk was assessed by calculating the Hazard Quotient (HQ) for each metal, defined as the ratio of the estimated daily intake (EDI) to the reference dose (RfD), using standard ingestion rates for adults (0.1 kg/day) and children (0.2 kg/day) [17].

Pilot-scale remediation trial: The effectiveness of pH correction and soil additions for immobilizing heavy metals throughout the dry season was assessed by pilot-scale remediation studies (March 2025). At Site-A, three 1 m^2 plots were treated with bentonite clay (5% w/w), biochar made from rice husk (5% w/w) and lime ($CaCO_3$) to elevate the soil pH to 7.0-7.5. To encourage reactivity, 2 t/ha of lime was added, blended into the top 10 cm of soil and watered. In order to assure cost-effectiveness, biochar was purchased locally and combined with bentonite in a similar manner [18,19]. No changes were made to the control plots. Composite soil samples (0-10 cm) were taken after 30 days and ICP-MS and 0.01 M $CaCl_2$ extraction were used to check for bioavailable metals. To evaluate the effects of amendments, changes in soil pH and CEC were assessed [11]. Biochar was prepared from rice husk through pyrolysis at 500 ºC under oxygen-controlled conditions. Commercially available bentonite clay was procured and used directly without any further pretreatment or modification.

Statistical analysis: All experiments were performed in triplicate and statistical analyses were performed using GraphPad Prism version 7.04 statistical software. Two-way analysis of variance (ANOVA) was done to compare the difference between sites and seasons. The difference was considered significant at p-value ≤ 0.05. It should be noted that although seasonal fluctuations were mainly assessed using XRD and geochemical data, SEM and XPS investigations were performed on representative samples under ambient conditions to establish baseline features.

RESULTS AND DISCUSSION

Soil and waste properties: Analysis of soil and waste properties revealed distinct characteristics across the three sampling sites (site A: jarosite rich waste dump; site B: adjacent agricultural soil; site C: uncontaminated reference soil) and between the wet and dry seasons. As summarised in Table-1, soil pH exhibited a significant (p < 0.005) range from 5.44 at site A to 7.04 ± 0.18 at site C. Site A consistently demonstrated higher acidity, with pH values averaging 5.44 ± 0.08 in the dry season and slightly increasing to 5.76 ± 0.08 in the wet season, a direct consequence of the presence and weathering of jarosite residue. In contrast, site B maintained a nearly neutral pH (averaging 6.14 ± 0.16 in dry season and 6.2 ± 0.2 in wet season), while site C, the uncontaminated reference site, showed a slightly alkaline pH (averaging 7.04 ± 0.18 in dry season and 7.06 ± 0.11 in wet season), reflecting natural soil conditions in the region. The electrical conductivity (EC) measurements further highlighted the impact of the industrial waste. site A recorded significantly (p < 0.005) elevated EC values, ranging from 2.624 ± 0.5 mS/cm in dry season to 2.16 ± 0.23 in wet season, indicative of high sulphate content originating from jarosite residue dissolution. This contrasts sharply with site C, which exhibited low EC values (0.38 ± 0.06 mS/cm in dry season while 0.396 ± 0.01 in wet season), typical of uncontaminated soils. Site B showed intermediate EC values (1.176 ± 0.26 mS/cm in dry season while 1.142 ± 0.21 mS/cm during wet season), suggesting some influence from the nearby waste dump. Seasonal variations in EC were also observed, with wet season samples generally showing slightly lower EC values, likely due to the diluting effect of increased rainfall [6].

Organic carbon content was consistently low across all sites, typically less than 0.8%, which is characteristic of the sandy loam soils prevalent in the Dariba region and consistent with the previous observations [20]. Cation exchange capacity (CEC) varied from 8.7 ± 0.33 to 11.34 ± 0.41 cmol/kg. Site A displayed the lowest CEC values (8.7 ± 0.33 in dry season while 8.88 ± 0.53 cmol/kg in wet season), primarily attributable to its low clay content and the dominance of mineral waste. Sites B and C showed progressively higher CEC values (10.16 ± 0.46 and 11.34 ± 0.41 cmol/kg, respectively in dry season while 10.56 ± 0.39 and 11.12 ± 0.45 cmol/kg, respectively in wet season) (p < 0.005), reflecting their higher soil

TABLE-1
PHYSICO-CHEMICAL PROPERTIES OF SOIL SAMPLES COLLECTED FROM DIFFERENT SITES ACROSS SEASONS

Season	Site	pH	EC (mS/cm)	Organic carbon (%)	CEC (cmol/kg)
Dry season	Site A	5.44 ± 0.08	2.624 ± 0.5	0.62 ± 0.12	8.7 ± 0.33
	Site B	6.14 ± 0.16*	1.176 ± 0.26*	0.624 ± 0.118	10.16 ± 0.46*
	Site C	7.04 ± 0.18*	0.38 ± 0.06*	0.604 ± 0.1	11.34 ± 0.41*
Wet season	Site A	5.76 ± 0.08	2.16 ± 0.23	0.512 ± 0.11	8.88 ± 0.53
	Site B	6.2 ± 0.2*	1.142 ± 0.21*	0.556 ± 0.16	10.56 ± 0.39*
	Site C	7.06 ± 0.11*	0.396 ± 0.01*	0.558 ± 0.13	11.12 ± 0.45*

**Value represented as Mean ± SD. *p < 0.005 in comparison to site A in same season.

organic matter and clay content, which contribute to higher metal retention capacity.

Mineralogical studies: XRD analysis confirmed the dominance of jarosite residue at site A, the industrial waste dump, with rietveld analysis indicating its abundance ranging from 70% to 85%. Alongside jarosite residue, goethite and anglesite were also detected, particularly in samples collected during the dry season (March 2025), with their proportions ranging from 5% to 10% and 3% to 8%, respectively (Table-2). This suggests a seasonal transformation of jarosite residue into these secondary phases. Notably, jarosite residue crystallinity, a measure of the order within its crystal lattice, was observed to be highest in the wet season samples (July 2025) and significantly declined in the dry season (Fig. 1). This reduction in crystallinity during the dry season is indicative of thermal-induced amorphisation and structural degradation of jarosite residue, consistent with findings from other studies on jarosite residue stability under varying environmental conditions [17,21]. In contrast, sites B (adjacent agricultural soil) and C (uncontaminated reference soil) showed no detectable presence of jarosite residue. Their mineralogical composition was dominated by quartz (60-70%) and various clay minerals (20-30%), reflecting the natural geological background of the region. This clear distinction in mineralogy underscores the localised impact of the industrial waste on site A (Table-2).

Based on the SEM micrographs (Fig. 2), jarosite residue minerals have semi-rhombohedral shape and aggregated, irregular crystalline structures. The observed particle aggregation along with their rough and porous surfaces indicates gradual structural alterations induced by seasonal environmental stressors. Partial transformation and surface modification processes are reflected in this aggregated morphology. The observed surface roughness and particle aggregation are comparable with the reduced crystallinity revealed in XRD analysis, indicating a slow degradation of the structure over the dry season. The XRD-derived decrease in crystallinity is supported by SEM micrographs (Fig. 2a-d), which show aggregated morphologies, irregular particle shapes and surface roughness.

Chemical composition: The presence of Fe, S, O, Na, Si and Al in the jarosite residue sample was verified by XPS analysis (Fig. 3). These elements correlate to distinctive peaks in the survey spectrum (Fig. 3a). The existence of Fe^{3+} species in the jarosite residue structure is confirmed by high-resolution spectra that show Fe $2p_{3/2}$ and Fe $2p_{1/2}$ peaks at ~710 eV and ~724 eV, respectively, verifying the existence of Fe^{3+}. Sulphate (SO_4^{2-}) groups are identified by the S 2p peak at around 168 eV, while oxygen in hydroxyl and sulphate structures is represented by the O 1s peak at about 531 eV. The integration of Na in the jarosite structure is confirmed by the Na 1s peak at around 1071 eV. The jarosite residue composition and silicate impurities are supported by the XPS quantification (Table-3), which reveals a predominant oxygen concentration with little Fe and S [22]. Surface contamination during sample processing is responsible for the comparatively high carbon content.

TABLE-2
MINERALOGICAL COMPOSITION OF SOIL SAMPLES COLLECTED FROM DIFFERENT SITES ACROSS SEASONS

Site	Season	Jarosite residue (%)	Goethite (%)	Anglesite (%)	Quartz (%)	Clay minerals (%)	Jarosite residue crystallinity
Site A	Wet	75.6	4.9	2.5	3.0	0.8	0.87
Site A	Dry	70.9	9.3	6.0	3.5	0.1	0.8
Site B	Wet	0.8	0.2	0.2	61.8	23.0	ND
Site B	Dry	0.5	0.4	0.3	66.1	21.4	ND
Site C	Wet	0.3	0.4	0.5	67.9	22.0	ND
Site C	Dry	0.5	0.6	0	66.1	21.7	ND

*ND = Jarosite residuenot detected in XRD, crystallinity not applicable.

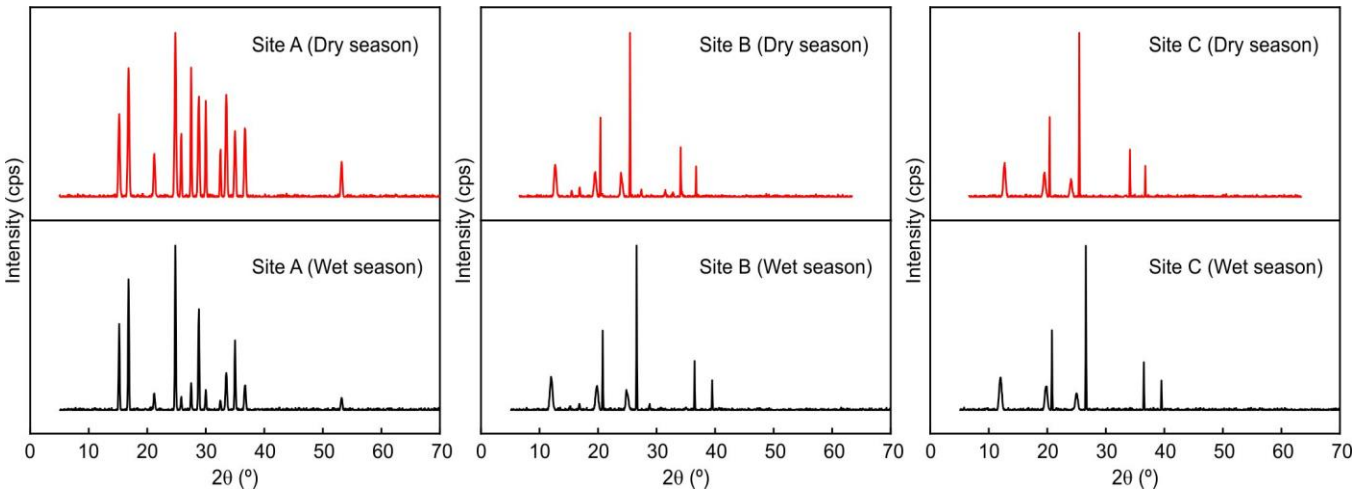

Fig. 1. XRD patterns of soil and jarosite-rich trash samples from Site A (dump), Site B (near agricultural soil) and Site C (reference soil) throughout wet and dry seasons

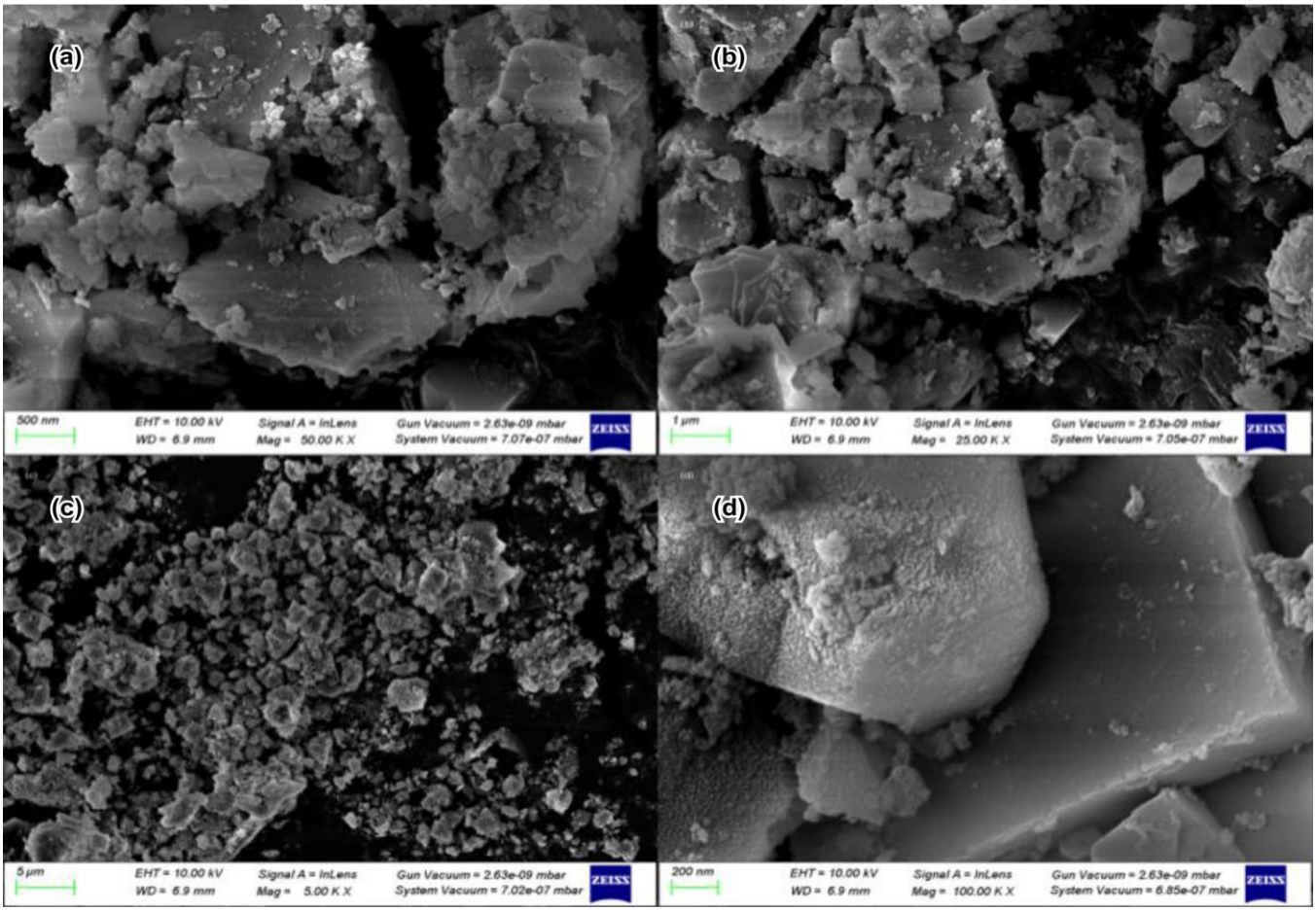

Fig. 2. SEM micrographs of jarosite residue at different magnifications showing (a) particle aggregation, (b) irregular morphology (c) crystalline structure and (d) surface roughness and porosity

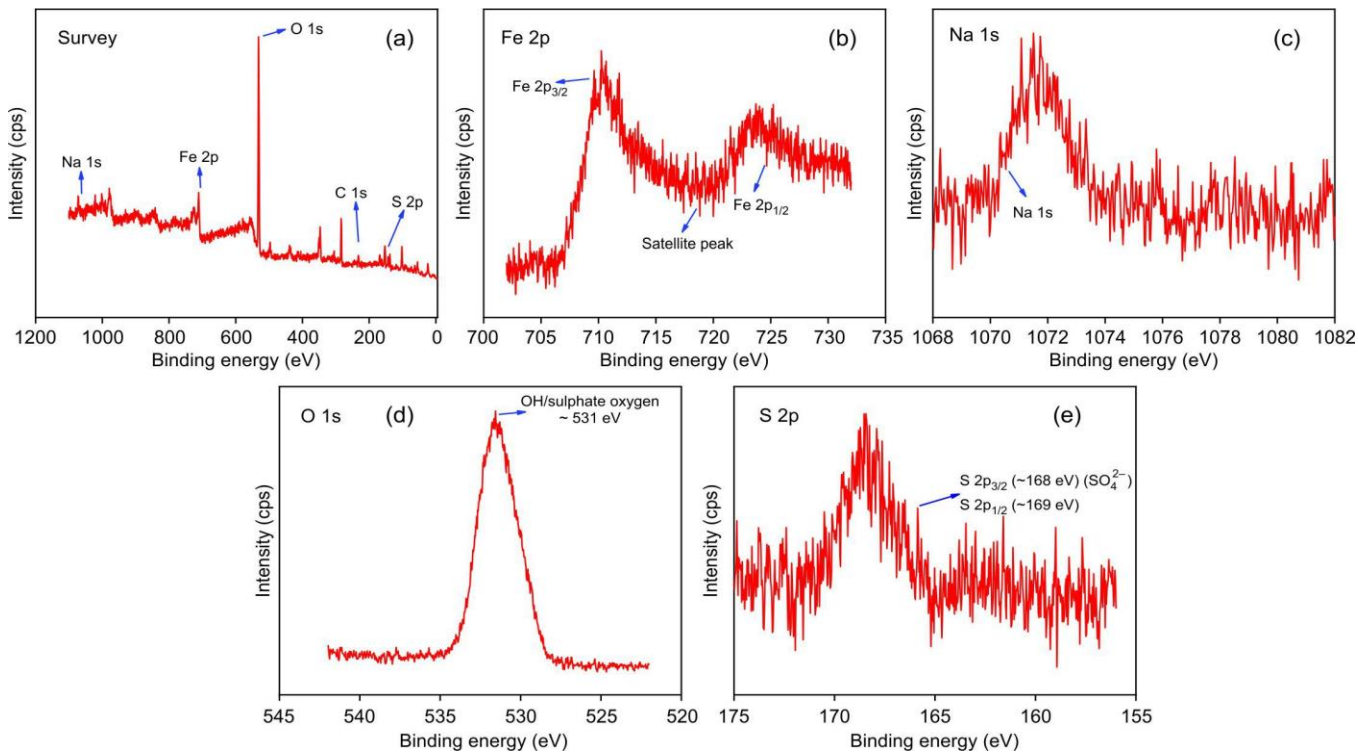

Fig. 3. XPS spectra of jarosite residue showing (a) survey spectrum and high-resolution spectra of (b) Fe 2p, (c) S 2p, (d) O 1s and (e) Na 1s

TABLE-3
SURFACE ELEMENTAL COMPOSITION OF THE JAROSITE RESIDUE SAMPLE DETERMINED BY XPS

Element	Binding energy (eV)	Atomic (%)
O 1s	~531	42.91
C 1s	~284	24.90
Si 2p	~102	16.39
Ca 2p	~347	4.58
Al 2p	~74	3.48
S 2p	~168	3.37
Fe 2p	~710	2.84
Na 1s	~1071	1.53

Seasonal control and dissolution mechanism: The findings of the combined morphological and batch dissolution show that temperature and pH have a significant influence on jarosite residue stability. Significant metal leakage (Pb ~70%, As ~54%) was seen under dry-season circumstances (pH 7.5, 45 ºC). Although XPS verifies chemical stability at the surface, XRD and SEM show structural disorder and morphological deterioration, suggesting that the main cause of heavy metal release is crystallinity loss rather than compositional change. Moreover, arsenic mobilisation is facilitated by sulphate–arsenate exchange [23].

Heavy metal speciation: Inductively coupled plasma mass spectrometry (ICP-MS) analysis revealed significant variations in the total concentrations of heavy metals across the sampling sites as detailed in Table-4. Site A, the jarosite residue-rich waste dump, exhibited markedly elevated concentrations of Fe, Zn, Pb, As and Cd. Specifically, over both the seasons span average concentrations at site A were 23.9 ± 0.08% for Fe, 7.9 ± 0.04% for Zn, 2.3 ± 0.008% for Pb, 0.79 ± 0.004% for As and 0.19 ± 0.0019% for Cd. These values are substantially higher than those observed at site B (adjacent agricultural soil), which had lower concentrations and site C (uncontaminated reference soil), where only trace levels of these metals were detected. The localised effects of the mining waste on the ecosystem are observed in this gradient in metal concentrations. Analytical accuracy was confirmed by recovery values for verified reference materials, which varied from 92% to 105% [23].

To understand the mobility and potential bioavailability of the heavy metals, the Community Bureau of Reference (BCR) sequential extraction procedure was applied to samples from site A. Pb and As were focused-on pertaining to their high concentration levels, strong seasonal variability and environmental relevance, while Cd was included due to its known high mobility in soil systems. The results, presented in Table-5, provide insights into the speciation of Pb, As and Cd across four fractions *viz*. acid-soluble, reducible, oxidisable and residual. In the wet season, Pb and As were predominantly found in the residual fraction (65-75%), indicating their strong binding within stable mineral phases, likely jarosite residue. However, a significant shift was observed in the dry season, with 45-55% of Pb and As migrating to the more mobile acid-soluble and reducible fractions ($p < 0.01$). This shift suggests a decrease in the stability of the metal-bearing phases, leading to an increased risk of environmental release. In both seasons, Cd exhibited higher mobility, with 25-35% present in the acid-soluble fraction, reflecting its weaker association with the solid matrix compared to Pb and As [14].

Bioavailable concentrations were determined only in case of Pb and As, as these metals posed the highest environmental concern and presented the most pronounced reaction to season changes. The bioavailability of Pb and As at site A was observed to be highly sensitive to seasonal variations, as indicated in Table-6. Bioavailable concentrations of Pb were much higher at site A in the dry season (19.52 ± 1.37 mg/kg) than the wet season (5.59 ± 0.93 mg/kg). Similarly, bioavailable

TABLE-4
TOTAL HEAVY METAL CONCENTRATIONS (%) IN SOIL SAMPLES COLLECTED FROM DIFFERENT SITES ACROSS SEASONS

Metals	Season	Site A	Site B	Site C
Fe	Wet season	24.0140 ± 0.0848	2.0498 ± 0.0694***	0.9816 ± 0.0606***
	Dry season	23.9661 ± 0.0767	1.9746 ± 0.0837***	1.0319 ± 0.0716***
Zn	Wet season	7.8973 ± 0.0486	0.8005 ± 0.0451***	0.2009 ± 0.0106***
	Dry season	7.9062 ± 0.0556	0.8262 ± 0.0197***	0.1967 ± 0.0103***
Pb	Wet season	2.3040 ± 0.0029	0.2977 ± 0.0079***	0.03002 ± 0.0009***
	Dry season	2.2986 ± 0.0112	0.3021 ± 0.0082***	0.02902 ± 0.0005***
As	Wet season	0.7968 ± 0.0066	0.1016 ± 0.0049***	0.01016 ± 0.0007***
	Dry season	0.7970 ± 0.0032	0.0987 ± 0.0014***	0.01020 ± 0.0001***
Cd	Wet season	0.1986 ± 0.0018	0.0198 ± 0.0031***	0.00301 ± 0.00004***
	Dry season	0.1989 ± 0.0021	0.0188 ± 0.0018***	0.00295 ± 0.00006***

Values are represented as Mean ± SD. ***$p < 0.005$ in comparison to site A in same season.

TABLE-5
DISTRIBUTION OF HEAVY METAL FRACTIONS IN SITE A SOIL BASED ON THE BCR SEQUENTIAL EXTRACTION PROCEDURE

Site	Season	Metal	Acid-soluble (%)	Reducible (%)	Oxidizable (%)	Residual (%)
Site A	Wet season	Pb	13.0	10.9	5.3	74.5
		As	14.8	14.0	6.5	66.0
		Cd	31.8	24.4	15.6	25.0
	Dry season	Pb	20.2	29.5	11.3	41.6
		As	21.6	27.6	12.7	36.8
		Cd	34.7	27.8	19.7	28.9

TABLE-6
BIOAVAILABLE HEAVY METAL CONCENTRATIONS ACROSS COLLECTION SITES AND SEASONS

Metals	Season	Site A	Site B	Site C
Pb (mg/kg)	Wet season	5.59 ± 0.93	2.41 ± 0.21	0.048 ± 0.0048
	Dry season	19.52 ± 1.37	7.79 ± 0.76	0.052 ± 0.0093^{ns}
As (mg/kg)	Wet season	2.08 ± 0.21	1.38 ± 0.26	0.029 ± 0.0047
	Dry season	7.74 ± 0.9	2.88 ± 0.46	0.035 ± 0.0088^{ns}

All value were significant with $p < 0.0005$ except marked ns. Values are presented as Mean ± SD.

TABLE-7
HEAVY METAL RELEASE DURING BATCH DISSOLUTION EXPERIMENTS UNDER DIFFERENT EXPERIMENTAL CONDITIONS

pH	Temperature (ºC)	Time (h)	Pb release (%)	As release (%)	Cd release (%)	Zn release (%)
5.5	10	24	6.1	8.9	6.2	4.8
	10	48	5.5	6.5	4.2	5.6
	45	24	32.0	39.2	15.3	24.5
	45	48	36.6	29.2	17.7	12.8
7.5	10	24	26.1	35.5	21.5	14.4
	10	48	32.2	27.8	19.4	15.5
	45	24	69.8	55.1	41.0	37.6
	45	48	70.4	52.2	43.0	35.9

concentration of As increased from 2.08 ± 0.21 mg/kg in the wet season to 7.74 ± 0.9 mg/kg in the dry season. Site B exhibited moderate bioavailability, while site C had negligible extractable metals, further emphasizing the localised contamination.

Batch dissolution experiments: Batch dissolution experiments were conducted to simulate the seasonal conditions and to directly assess the stability of jarosite residue and the release of heavy metals under controlled parameters. The results, presented in Table-7, demonstrate a clear correlation between environmental conditions (pH and temperature) and the extent of metal release. Dissolution was found to be highest under conditions simulating the dry season, specifically at pH 7.5 and 45 ºC. Under these conditions, a significant proportion of heavy metals was released from the jarosite residue-rich samples, with approximately 70% of Pb and 54% of As being released within 48 h. This high release is a result of oxidation of jarosite residue to more soluble secondary phases, predominantly goethite. On the other hand, in a wet season-like condition (pH 5.5 and 10 ºC), the dissolution of jarosite residue was minimal and the release of metal was less than 8% of all the heavy metals tested. This shows the stabilizing nature of the low temperatures and acidic conditions on jarosite residue as could be anticipated of its formation conditions. Interestingly, even under these minimal dissolution conditions, a slight increase in As mobility was observed at pH 5.5, which can be attributed to sulphate-arsenate exchange mechanisms, where arsenate ions compete with SO_4^{2-} ions for binding sites within the mineral structure, leading to its release into the solution [5]. The batch dissolution experiments were consistent with the field observations, confirming that dry-season conditions promote enhanced dissolution of jarosite residues and increased release of associated heavy metals. Elevated temperatures and higher pH conditions, resulting from reduced rainfall and intensified evaporation, were found to significantly influence metal mobilization. Table-7 further demonstrate the strong dependence of heavy metal release on both temperature and pH, highlighting their critical role in governing contaminant mobility and environmental risk.

Crop metal accumulation and human health risk assessment: Analysis of wheat and maize grains from site B revealed significant heavy metal accumulation, with higher concentrations in the dry season crop (Table-8). In dry season, wheat grains were found to have heavy metal accumulation 2.5 ± 0.2 mg/kg Pb, 0.9 ± 0.1 mg/kg As and 0.3 ± 0.02 mg/Kg Cd. Meanwhile in the wet season, maize grains present an accumulation of 1.2 ± 0.1 mg/kg Pb, 0.7 ± 0.1 mg/kg As and 0.2 ± 0.03 mg/kg.

TABLE-8
HEAVY METAL ACCUMULATION IN WHEAT AND MAIZE GRAINS FROM SITE B (mg/kg DRY WEIGHT)

Metal	Wheat	Maize
Pb (mg/kg)	2.5 ± 0.20	1.2 ± 0.10
As (mg/kg)	0.9 ± 0.10	0.7 ± 0.10
Cd (mg/kg)	0.3 ± 0.02	0.2 ± 0.03

Bioaccessibility assessment (Table-9) revealed that approximately 40-50% of Pb, As and Cd present in cereal grains were potentially available for gastrointestinal absorption. Furthermore, the calculated Hazard Quotient (HQ) values (Table-10) indicated significant non-carcinogenic health risks, particularly for children. Wheat consumption exhibited HQ values of 1.8 for Pb and 1.3 for As, while maize consumption showed HQ values of 1.4 and 1.0 for Pb and As, respectively. Since HQ values equal to or greater than 1 indicate potential adverse health effects, these findings underscore the health risks associated with long-term dietary exposure to contaminated grains [12].

TABLE-9
BIOACCESSIBLE HEAVY METAL CONCENTRATIONS IN CROPS AT SITE B

	Wheat	Maize
Pb (mg/kg)	1.2	0.90
As (mg/kg)	0.4	0.30
Cd (mg/kg)	0.1	0.08

TABLE-10
HAZARD QUOTIENT (HQ) FOR HEAVY METALS IN CROPS

	Wheat		Maize	
	Adult	Child	Adult	Child
Pb HQ	0.9	1.8	0.7	1.4
As HQ	0.7	1.3	0.5	1.0
Cd HQ	0.2	0.4	0.1	0.3

Pilot-scale remediation trials: Pilot-scale trials demonstrated significant reductions in bioavailable metals (Table-11) at site A during the dry season. Lime treatment increased soil pH from 5.5 to 7.2, reducing bioavailable Pb by 60% (from 16.5 to 6.6 mg/kg), As by 55% (from 6.6 to 3.0 mg/kg) and Cd by 57% (from 2.1 to 0.9 mg/kg). Biochar treatment increased soil pH from 5.5 to 6.0, reducing bioavailable Pb by 65% (from 16.5 to 5.8 mg/kg), As by 61% (from 6.6 to 2.6 mg/kg) and Cd by 62% (from 2.1 to 0.8 mg/kg). Bentonite amendments were equally effective, as it increased soil pH from 5.5 to 6.2, reducing Pb by 62% (from 16.5 to 6.3 mg/kg), As by 58% (from 6.6 to 2.8 mg/kg) and Cd by 57% (from 2.1 to 0.9 mg/kg). Lime and bentonite treatments resulted in a slight increase in EC due to the release of soluble ions; however, both amendments remained cost-effective and demonstrated strong potential for large-scale field application.

TABLE-11
BIOAVAILABLE HEAVY METAL CONCENTRATIONS POST-REMEDIATION (DRY SEASON, SITE A)

	Control	Lime	Biochar	Bentonite
pH	5.5	7.2	6.0	6.2
CEC (cmol/kg)	8.7	9.0	10.4	9.8
Pb (mg/kg)	16.5	6.6	5.8	6.3
As (mg/kg)	6.6	3.0	2.6	2.8
Cd (mg/kg)	2.1	0.9	0.8	0.9

Conclusion

This study demonstrated that seasonal environmental conditions strongly influence the stability of jarosite residues and the mobility of associated heavy metals in the Dariba mining region. XRD, SEM and XPS analyses revealed progressive structural degradation of jarosite during the dry season, accompanied by increased release of Pb, As and Cd. The sequential extraction and bioavailability studies showed a seasonal shift of Pb and As from stable mineral-bound forms to more mobile fractions, thereby increasing their environmental availability. Batch dissolution experiments confirmed that increased temperature (45 ºC) and nearly neutral pH significantly enhanced jarosite dissolution, resulting in the release of up to 70% Pb and 54% As. Consistent with these findings, agricultural soils and crops located near the waste dump exhibited elevated metal concentrations. Bioaccessibility assessments indicated that 40-50% of Pb, As and Cd in cereal grains were potentially available for human absorption, while Hazard Quotient values < 1 for Pb and As highlighted potential non-carcinogenic health risks, particularly for children. Pilot-scale remediation trials demonstrated that lime, biochar and bentonite effectively reduced heavy metal bioavailability, with biochar showing the highest immobilization efficiency. This study highlights the importance of implementing cost-effective remediation measures to reduce environmental contamination and protect human health in mining-affected regions.

ACKNOWLEDGEMENTS

The authors sincerely thank Dr. P.B. Saxena, HOD, Department of Chemistry, Allen Career Institute for his invaluable support. One of the authors, Akhtar extends special appreciation to Mr. Vijay Soni (Senior Vice-President, Allen Career Institute), Mr. Vinit Gangwal and Mr. Yogesh Malav (Vice President, Allen Career Institute) for their generous assistance and contributions.

CONFLICT OF INTEREST

The authors declare that there is no conflict of interests regarding the publication of this article.

DECLARATION OF AI-ASSISTED TECHNOLOGIES

During the preparation of this manuscript, the authors used an AI-assisted tool(s) to improve the language. The authors reviewed and edited the content and take full responsibility for the published work.

REFERENCES

1. A. Pappu, M. Saxena and S.R. Asolekar, *Build. Environ.*, **42**, 2311 (2007); https://doi.org/10.1016/j.buildenv.2006.04.015
2. J. Bech, *Environ. Geochem. Health*, **42**, 4065 (2020); https://doi.org/10.1007/s10653-020-00741-w
3. I. Thornton, *Sci. Total Environ.*, **198**, 105 (1997); https://doi.org/10.1016/S0048-9697(97)05434-X
4. C.G. Weisener, M.G. Babechuk, B.J. Fryer and C.J.G. Maunder, *Geobiology*, **6**, 415 (2008); https://doi.org/10.1111/j.1472-4669.2008.00167.x
5. M.P. Asta, J. Cama, M. Martínez and J. Giménez, *J. Hazard. Mater.*, **171**, 965 (2009); https://doi.org/10.1016/j.jhazmat.2009.06.097
6. A. Kumar and P.R. Golani, *Geoheritage.*, **15**, 80 (2023); https://doi.org/10.1007/s12371-023-00837-6
7. A.K. Sinha, V.G. Havanagi and J.T. Shahu, *Int. J. Pavement Eng.*, **22**, 882 (2021); https://doi.org/10.1080/10298436.2019.1652299
8. M. Zhu, Y. Wang, C. Zheng, Y. Luo, Y. Li, S. Tan, Z. Sun, Y. Ke, C. Peng and X. Min, *J. Environ. Manage.*, **370**, 122396 (2024); https://doi.org/10.1016/j.jenvman.2024.122396
9. M. Qasim, S. Manzoor, M.I. Nabeel, Q. Ullah, Y.Z. Sair, T. Khomphet, C.G. Joseph, A. Raza, J. Suazo-Hernández and T. Gulzar, *Front. Sustain.*, **7**, 1777462 (2026); https://doi.org/10.3389/frsus.2026.1777462
10. B.R. Shetty, P.B. Jagadeesha and S.A. Salmataj, *CYTA J. Food*, **23**, 2438726 (2025); https://doi.org/10.1080/19476337.2024.2438726.
11. M.E. Sumner and W.P. Miller, in eds.: D.L. Sparks, A.L. Page, P.A. Helmke, R.H. Loeppert, P.N. Soltanpour, M.A. Tabatabai, C.T. Johnston and M.E. Sumner, Cation Exchange Capacity and Exchange Coefficients, In: Methods of Soil Analysis: Part 3–Chemical Methods, Eds. Madison, WI, USA: Soil Science Society of America, pp. 1201-1229 (1996).
12. S.M. Fortier, N.T. Nassar, K.D. Kelley, G.W. Lederer, J.L. Mauk, J.M. Hammarstrom, W.C. Day and R.R. Seal II, *Mining Engineer.*, **73**, 48 (2021).
13. M. Xiang, Y. Li, J. Yang, K. Lei, Y. Li, F. Li, D. Zheng, X. Fang and Y. Cao, *Environ. Pollut.*, **278**, 116911 (2021); https://doi.org/10.1016/j.envpol.2021.116911

14. O.S. Shokunbi, O.O. Ajayi, D.O. Jegede and O.S. Shokunbi, *Int. J. Human Capital Urban Manage.*, **5**, 339 (2020); https://doi.org/10.22034/IJHCUM.2020.04.06
15. C. Drouet and A. Navrotsky *Geochim. Cosmochim. Acta*, **67**, 2063 (2003); https://doi.org/10.1016/S0016-7037(02)01299-1
16. S.M. Rodrigues, N. Cruz, L. Carvalho, A.C. Duarte, E. Pereira, A.G.F. Boim, L.R.F. Alleoni and P.F.A.M. Römkens, *Sci. Total Environ.*, **635**, 188 (2018); https://doi.org/10.1016/j.scitotenv.2018.04.063
17. H.R. Boostani, M. Najafi-Ghiri and D. Khalili, *Sci. Rep.*, **15**, 14301 (2025); https://doi.org/10.1038/s41598-025-99120-7
18. H. Gong, L. Zhao, X. Rui, J. Hu and N. Zhu, *J. Hazard. Mater.*, **432**, 128668 (2022); https://doi.org/10.1016/j.jhazmat.2022.128668
19. S. Beesley, E. Moreno-Jiménez, J.L. Gomez-Eyles, B. Robinson, E. Harris and T. Sizmur, *Environ. Pollut.*, **159**, 3269 (2011); https://doi.org/10.1016/j.envpol.2011.07.023
20. R. Miller and L. Sonon, in eds.: F.J. Sikora and K.P. Moore, Nitrate nitrogen, In: Soil Test Methods from the Southeastern United States, Southern Cooperative Series Bulletin No. 419, pp. 155-157 (2014).
21. A. Narsimha and J. Wu, *Hum. Ecol. Risk Assess.*, **25**, 191 (2019); https://doi.org/10.1080/10807039.2018.1546550
22. V. Akhtar and D. Kulhary, *Asian J. Chem.*, **37**, 1995 (2025); https://doi.org/10.14233/ajchem.2025.33897
23. N. Saha and A.S. Majumdar, Abstract no. EGU26-12992, Integrated Micro to Nano-Scale Characterization of Hydrous Sulphate Mineral–Jarosite in Kachchh, Gujarat, India: Implication for Mars, EGU General Assembly 2026, Vienna, Austria, May 3-8 (2026); https://doi.org/10.5194/egusphere-egu26-12992
24. R.S. Shekhawat, P. Kushwaha and M. Agarwal, *Innov. Infrastruct. Solut.*, **11**, 151 (2026); https://doi.org/10.1007/s41062-026-02567-4